

Numerical Weather Models for Tropospheric Mitigation in Marine Kinematic GPS: a Daylong Analysis

Felipe G. Nievinski

Department of Geodesy and Geomatics Engineering, University of New Brunswick, Canada

BIOGRAPHY

Felipe Nievinski is a M.Sc.E. student and research assistant at the Dept. of Geodesy and Geomatics Engineering, University of New Brunswick. At the end of 2004 he received his degree in Geomatics Engineering from the Federal University of Rio Grande do Sul, Brazil. He is a member of the Institute of Navigation, the American Geophysical Union, and the Society for Industrial and Applied Mathematics.

ABSTRACT

It has been recommended that, “in precise [static] applications where millimetre accuracy is desired, the delay must be estimated with the other geodetic quantities of interest” [McCarthy and Petit, 2004, p. 100]. While that recommendation is common practice in static positioning, tropospheric delay remains as one of the main error sources in medium to long-distance kinematic positioning. Its mitigation is more challenging in kinematic applications because its strong correlation with the vertical coordinate is aggravated by the need to estimate the rover position at every epoch.

In this paper we report one further step in our investigation on the use of Numerical Weather Models (NWM) for predicting tropospheric delays, aiming at improvements in kinematic applications. We analyze a daylong session. Our results show that NWM yields a slight improvement in height bias, with no improvement in horizontal bias. Observation residuals show no significant change.

We have shown that NWM have only marginal improvement on a 70 km kinematic baseline over well-established, simpler, tropospheric delay prediction models (Saastamoinen, UNB3m). As ray-tracing in NWM is far more complex and computationally more expensive than those simpler models, they should be preferred until one demonstrates that the impact in using NWM tropospheric delay predictions is, indeed, far superior.

INTRODUCTION

GPS radio signals are refracted when they propagate through the Earth's neutral atmosphere (the bulk of which is the troposphere but also includes the stratosphere). Timing (ranging) of GPS signals is delayed (increased) compared to what would be measured if the signals propagated in a vacuum. In other words, the distance measured with GPS signals propagating through the neutral atmosphere is always greater than the geometrical distance between satellite's and receiver's antennas. The delays (hereafter tropospheric delays) range from 2.3 m at zenith to approximately 26 m at 5° elevation-angle, for a station on the geoid [Seeber, 2003].

It has been recommended that, “in precise [static] applications where millimetre accuracy is desired, the delay must be estimated with the other geodetic quantities of interest” [McCarthy and Petit, 2004, p. 100]. While that recommendation is common practice in static positioning, tropospheric delay remains as one of the main error sources in medium to long-distance kinematic positioning. Its mitigation is more challenging in kinematic applications because its strong correlation with the vertical coordinate is aggravated by the need to estimate the rover position at every epoch.

Whereas some authors recommend that the simultaneous estimation of position and tropospheric parameters be avoided [Schüler, 2006], others have tried to overcome this limitation [Dodson et al., 2001]. Both approaches would benefit from more realistic initial values for the troposphere, such as the ones given by Numerical Weather Models (hereafter NWM) [Cucurull et al., 2002].

NWM are generated by “the integration of the governing equations of hydrodynamics by numerical methods subject to specified initial conditions” [Glickman, 2000]. Global and regional NWP models are produced daily by several meteorological agencies throughout the world, mainly for weather forecasting purposes.

In addition, the marine environment poses unique challenges, due to, e.g., rapid-varying weather conditions and large gradients in pressure, temperature, and humidity from mainland to sea.

In this paper we report one further step in our investigation on the use of Numerical Weather Models for predicting tropospheric delays, aiming at improvements in kinematic applications. In the past, only 1 h [Nievinski et al., 2005; Ahn et al., 2006, Cucurull et al., 2002], 5 h [Cove et al., 2004], and 6 h [Jensen, 2002] kinematic sessions were analyzed; we speculate that is due to the large amounts of data that comprises NWM. In this paper we analyze a daylong session.

Our paper is organized as follows. First we describe the data used and the methods employed. Second we show and discuss the results obtained. The paper finishes with a summary of our findings.

DATA

We used dual-frequency GPS observations collected at 1 Hz sampling rate, over 1 full day, at 2 base stations and at one rover station. We downsampled the data to 30 s⁻¹ rate, in order to allow us to experiment with different processing settings in a timely manner. The rover is installed on a ferry boat (Figure 1) that goes back and forth across the Bay of Fundy, South-Eastern Canada, between the cities of Digby (N.S.) and St. John (N.B.), 75 km apart (Figure 2). The day selected was September 30, 2004, the most recent day for which we have full GPS data at the 3 stations, collected during the yearlong Princess of Acadia Project [Santos et al., 2004]. During that day the ferry crossed the bay 6 times.

We also used grids from the Canadian Global Environmental Multiscale Numerical Weather Model [Côté et al., 1998] (Figure 3). Its resolution is as follows: 15 km nominal (horizontal); 28 variable-height isobaric levels plus 1 ground level (vertical); 3 h (temporal). The NWM is initialized every 0 and 12 h UTC, at which 16 3-hourly grids are issued covering the following 48 h period. For the full day of September 30, 2004, we used the following grids (in the format initialization epoch + forecast intervals): September 30, 0 h +0,+3,+6,+9 h; September 30, 12 h +0,+3,+6,+9 h; and October 1st, 0 h +0 h.

We also used profiles of meteorological data (pressure, temperature, and relative humidity), collect by radiosondes launched from 89 sites over all of the NWM continental extent (Figure 4), at September 30, 0 h UTC.



Figure 1: Ferry boat employed as rover station.



Figure 2: Map of the base stations.

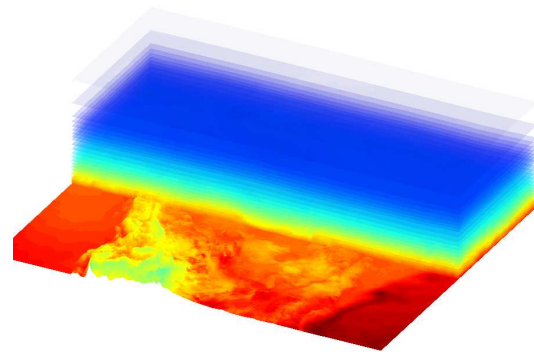


Figure 3: 3-dimensional refractivity field (unitless), as given by the Northern half of the GEM NWM. Height exaggerated 100 times.

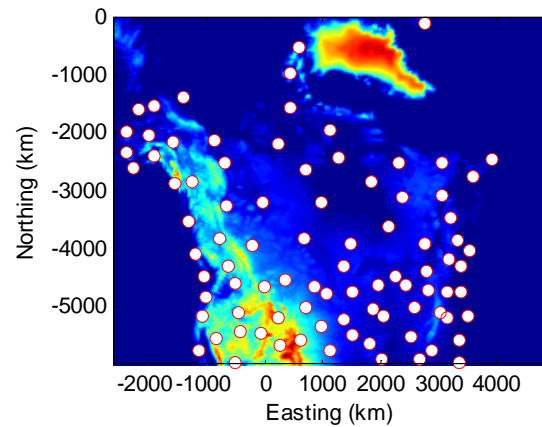


Figure 4: Location of the radiosonde launching sites.

METHODS

Generation of the NWM tropospheric delay predictions

We employed the ray-tracer described in Nievinski et al. [2005]. In the past, we have ray-traced directly slant delays; for this paper, we decided to ray-trace only zenith delays and map them to lower elevation angles using Niell's mapping function [Niell, 1996]. The motivation for that was to reduce the total ray-tracing processing time – in effect, we reduced it by a factor of 7, the mean number of visible satellites. The justification for that decision is that it is valid to study separately the delay at zenith and its elevation-angle dependence. Perhaps it is not only valid but also more useful, since it allows one to make separate conclusions about the usefulness of NWM for each aspect. In effect, we have put the study of the second aspect (see, e.g., Böhm and Schuh, 2004) outside the scope of this paper.

Generation of the GPS positioning results

We had two scenarios: one is the kinematic processing of a moving rover; another is the kinematic processing of a stationary rover. In each scenario we had (i) a reference solution and (ii) test solutions. Solution (i) should be more accurate and precise than any of (ii), so as to allow us to safely attribute any discrepancy between the two to errors in (ii).

In the stationary rover scenario, the test solutions were generated taking one of the base stations as rover. The reference solution comes from a weighted average of 5 static, precise point positioning daily solutions, spanning September 27 to October 1st, 2004 (inclusive).

The moving rover scenario is more challenging because, e.g., cycle slips will be more numerous and more difficult to detect and fix. The test solutions are the individual baseline solutions Digby-Ferry and St. John-Ferry. The reference solution is a multi-base station solution, in which the GPS observations collected at both base stations and at the Ferry are processed in the same Kalman filter. This multi-base station solution is better than processing each individual baseline separately and adjusting the ferry positions after the fact.

For the GPS kinematic processing, we employed NovAtel's (Waypoint Products Group) GrafNav Batch, version 7.60. We applied a 10° cut-off elevation angle, and satellites were weighted inversely proportional to the sine of their elevation angle. The L2 signal was used to help fix ambiguities. The L2 signal was also used to correct for ionospheric delay in all but the multi-base station solution – for discussion, please see section below.

We evaluated two tropospheric delay prediction models in addition to NWM: UNB3m [Leandro et al., 2006] and Saastamoinen with standard weather parameters reduced to the station height. For the multi-base station solution we employed the Saastamoinen model only. We did not estimate residual tropospheric delay in any kinematic solution.

For PPP processing, we employed the Canadian Spatial Reference System on-line PPP application¹. It predicts zenith tropospheric delay with Saastamoinen model as used in this paper, and also estimates residual tropospheric delay every epoch.

Validation of the NWM tropospheric delay predictions

To validate the NWM tropospheric delay predictions we compared them to radiosonde predictions. Radiosonde is often employed as benchmark in the validation of tropospheric delay prediction models (e.g., Mendes, 1999). It gives us hydrostatic and non-hydrostatic partial delays separately, allowing us to validate each component.

Validation of the GPS positioning results

We validated the GPS positioning results to assure we had reliable reference solutions vis-à-vis their respective test solutions. To do so, we checked the following two statistics: formal standard deviation and forward/reverse solution separation. Even though usually the reported formal standard deviations are too optimistic, we expect them to be consistently larger and smaller for worse and better solutions, respectively. The forward/reverse separation is the discrepancy between the two solutions given for the same baseline, obtained using exactly the same data and settings, as a feature of Kalman filters such as the one employed in GrafNav. Again, it is not exactly a measure of accuracy, but we expect it to be consistently larger and smaller for worse and better solutions, so as to allow us to use these statistics to draw a conclusion about the relative quality of reference and test solutions.

Assessment of the impact of NWM tropospheric delay predictions on the GPS positioning results

For both moving and stationary rover scenarios, we assessed the accuracy of the rover test solutions to the respective reference solutions. We also checked the phase and code measurement residuals.

¹ <http://www.geod.nrcan.gc.ca/ppp_e.php>

RESULTS AND DISCUSSION

Validation of the NWM tropospheric delay predictions

We compared NWM delays against radiosonde delays at the epoch September 30, 2004, 0 h UTC. We found centimetric biases and spread (summarized in Table 1), out of an average total delay amounting to 2.3 m.

Please notice in Figure 5 that the bias and spread in total delay correspond, respectively, to a bias in the hydrostatic component and to a spread in the non-hydrostatic component. The bias can be explained by an inaccurate transformation to geopotential heights, as part of the ray-tracing procedure. In the past we have found decimetric biases for this reason [Nievinski, 2005], which were fixed and reduced to the level presented here. The spread is expected for the non-hydrostatic delay, function of humidity hence highly variable and harder to predict. Also notice that the spread decreases towards higher latitudes; again, that is expected, since humidity in the air decreases towards the pole.

To further investigate the bias found in hydrostatic delay, we compared the NWM ray-traced value to the value obtained using Saastamoinen's formula and surface pressure as interpolated in the NWM (we call this NWM self-discrepancy in hydrostatic delay). Comparison results shown in Figure 6 resemble closely the discrepancies found in hydrostatic delay between NWM and radiosonde. That is an ongoing research issue.

Table 1: Statistics (in cm) for discrepancy between NWM and radiosonde delays.

	Mean	Rms	Std
Total Delay	1.05	1.29	0.75
Hydrostatic Delay	1.15	1.18	0.25
Non-Hydrostatic Delay	-0.1	0.69	0.69

Table 2: Statistics (in cm) for NWM self-discrepancy in hydrostatic delay.

	Mean	Rms	Std
Hydrostatic Delay	1.24	1.26	0.22

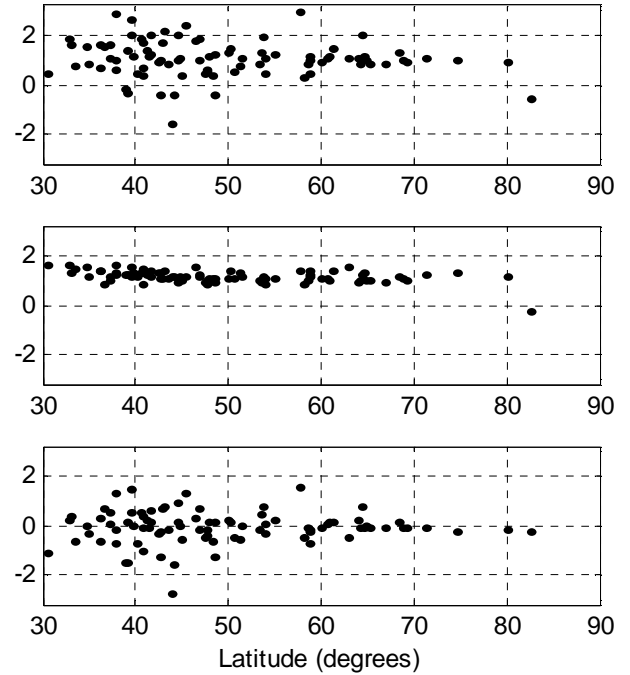


Figure 5: Discrepancy (in cm) between NWM and radiosonde delays. Top panel: total delay; Center panel: hydrostatic delay; Bottom panel: non-hydrostatic delay.

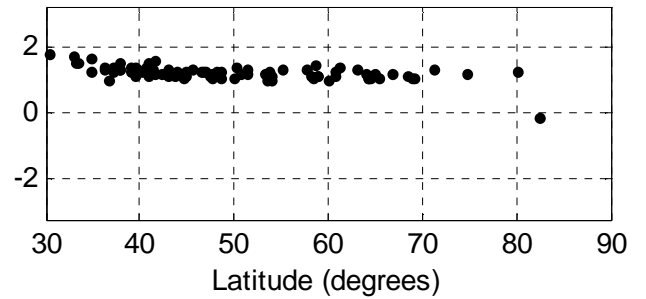


Figure 6: NWM self-discrepancy in hydrostatic delay (in cm).

Validation of the GPS positioning results – stationary rover scenario

The reference solution in the stationary rover scenario provides coordinates with millimetric repeatability and sub-millimetric formal standard deviations (Table 3), which we consider too optimistic. A more realistic figure is given by Kouba [2003], who demonstrates that with PPP and IGS products one can estimate station coordinates with centimetric accuracy.

Table 3: Base station coordinates.

	Height	Latitude	Longitude
Digby	37.4462 m	44° 37' 13.790254"	-65° 45' 34.9665"
(std)	2.0 mm	0.4 mm	0.9 mm
St. John	4.5362 m	45° 16' 17.54366"	-66° 03' 46.686244"
(std)	2.0 mm	0.6 mm	1.2 mm

We inspected the statistics for the test solutions (Table 4 and Table 5). We give statistics only for the baseline with Digby as base and St. John as rover because the second baseline (with exchanged base and rover) has values with nearly identical magnitude and biases with reversed sign. Since those figures are all larger than 1 cm, we concluded that the PPP solution can be used as a reliable reference in the stationary rover scenario.

Table 4: Rms (in cm) of forward/reverse separation; baseline with Digby as base and St. John as rover.

	Height	Latitude	Longitude
no model	51.8	21.1	26.4
Saastamoinen	9.6	6.6	5.7
UNB3m	6.9	3.7	3.7
NWM	7.0	3.8	3.8

Table 5: Formal standard deviations (in cm); baseline with Digby as base and St. John as rover.

	Height	Latitude	Longitude
no model	8.4	4.8	4.0
Saastamoinen	8.0	4.4	3.1
UNB3m	7.0	3.9	2.7
NWM	7.0	3.9	2.7

Validation of the GPS positioning results – moving rover scenario

First we inspected the forward/reverse separation and also the formal standard deviations (Table 6 and Table 7).

Table 6: Rms (in cm) of forward/reverse separation. (Leftmost column indicates base station).

		Height	Latitude	Longitude
St. John	no model	19.3	13.9	8.7
	Saastamoinen	14.8	7.3	6.3
	UNB3m	11.6	5.6	7.2
	NWM	15.6	5.9	5.4
Digby	no model	33.9	15.8	20.9
	Saastamoinen	6.5	3.9	3.7
	UNB3m	6.6	3.4	5.0
	NWM	6.4	3.4	4.7
Multi-base station		7.3	4.4	4.5

Table 7: Formal standard deviations (in cm). (Leftmost column indicates base station).

		Height	Latitude	Longitude
St. John	no model	7.3	4.0	2.8
	Saastamoinen	7.3	4.0	2.8
	UNB3m	6.7	3.7	2.6
	NWM	6.6	3.7	2.6
Digby	no model	6.4	3.6	2.7
	Saastamoinen	6.5	3.6	2.7
	UNB3m	6.0	3.3	2.4
	NWM	6.4	3.3	2.4
Multi-base station		3.6	2.1	1.5

The overall statistics are consistently better for the reference, multi-base solution, than for any of the test solutions. Yet, a closer inspection at the time series of those discrepancies reveals that, even though the multi-base station solution is almost always better than the individual baseline solutions, during certain periods it is not significantly better, as required for a reliable reference. For instance, Figure 7 shows that the height formal standard deviation for the multi-base station solution approaches that of NWM-corrected baseline solutions during certain periods.

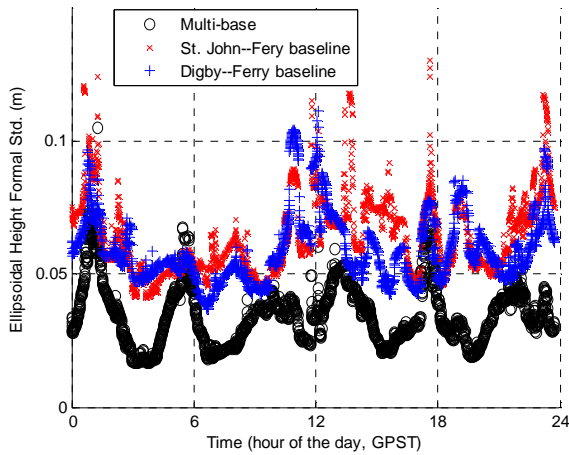


Figure 7: Time series of rover height formal standard deviation yielded by multi-base station and NWM-corrected individual baseline solutions.

Those periods can be defined based on the distance of the Ferry to the nearest base station (Figure 8). As expected, the closer the Ferry is to any base station, the better the multi-base station solution will be. Whenever that distance exceeds a certain threshold, the multi-base station solution, even though better, can no longer be relied upon as a reference solution for the individual baseline solutions. Empirically we have set that threshold value to 20 km.

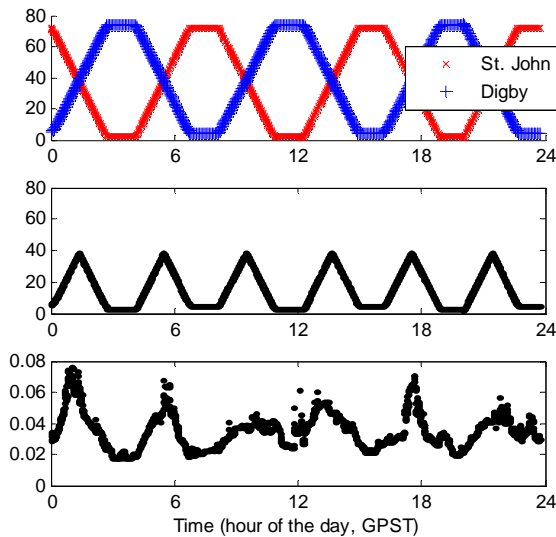


Figure 8: Top panel: distance from Ferry to either base station (in km); Center panel: distance from Ferry to nearest base station (in km); Bottom panel: height formal standard deviation for the multi-base station solution (m).

In addition to an upper distance threshold applied to the reference solution, we applied a lower distance threshold to the test solutions. The later is needed because we do not expect much different impact of different prediction models on short test baselines. As the Ferry goes back and forth between Digby and St. John, their respective individual baselines get shorter and longer, and the across-receiver observation differencing technique gets more and less effective in cancelling out the tropospheric delay common at both base and rover stations. While the length of a test baseline is smaller than a given threshold (baseline height offset being negligible), there is not much relative, residual, tropospheric delay left for the prediction models to correct for. Empirically we set that threshold value to 40 km.

To summarize, the combined criteria for meaningful discrepancies is that the distance to the nearest base station in the reference solution be smaller than 20 km, and the distance to the base station in the test solution be larger than 40 km. Figure 9 depicts that criteria graphically (contrast it with Figure 8, top and center panels). Please note we are intentionally discarding the epochs at which one could not draw conclusions about the impact of different tropospheric prediction models.

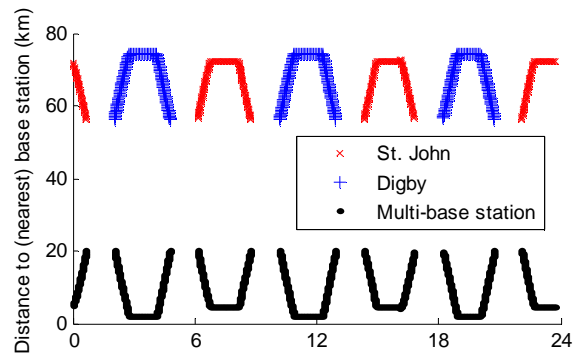


Figure 9: periods of each solution for which we can draw conclusions about the impact of different tropospheric prediction models.

Figure 9 also helps us explain why we decided to use L2 for ionospheric correction in the test solutions only, but not in the reference solution. The increased-noise ionospheric delay-free observable is beneficial for the individual long-baseline solutions, but would be unnecessary and even harmful in our multi-base station solution.

Impact assessment – stationary rover scenario

As in for its validation, we show results only for the baseline with Digby as base and St. John as rover. The corresponding figures would be flipped around the zeros axes.

NWM yields an improvement in height bias, with no improvement in horizontal bias. Scattering in longitude is slightly improved as well. Observation residuals surprisingly show no significant change, even when we use no tropospheric model.

Table 8: Rms of observation residuals (in m); stationary rover scenario.

	C/A Code	L1 Phase
no model	0.72	0.037
Saastamoinen	0.71	0.018
UNB3m	0.74	0.020
NWM	0.74	0.020

Table 9: Statistics for discrepancy (in cm) between test and reference solutions; stationary rover scenario.

	Height			Latitude			Longitude		
	mean	rms	std	mean	rms	std	mean	rms	std
no model	-7.8	25.2	23.9	8.2	13.7	11	2.6	17.2	17.0
Saastamoinen	-2.6	6.7	6.2	0.2	3.7	3.7	1.2	4.1	4.0
UNB3m	-2.5	6.0	5.4	0.2	3.2	3.2	1.2	2.7	2.4
NWM	-0.9	5.0	4.9	0.0	3.2	3.2	1.1	2.5	2.3

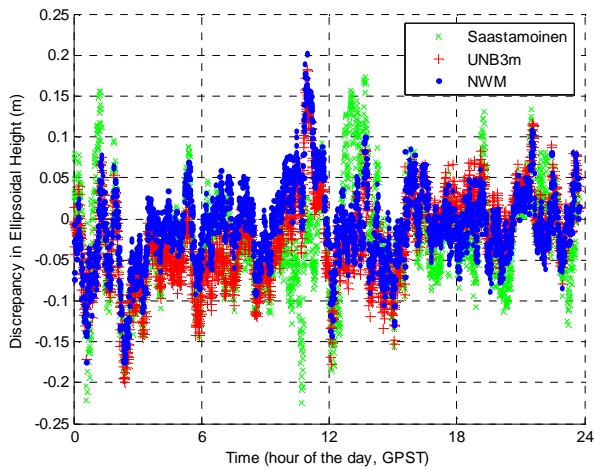


Figure 10: Time series of discrepancy in height; stationary rover scenario.

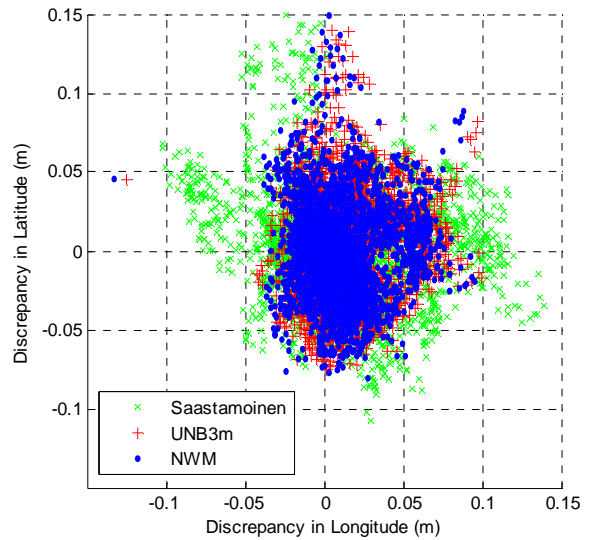


Figure 11: Horizontal discrepancy; stationary rover scenario.

Impact assessment – moving rover scenario

Overall, NWM improves the baseline St. John–Ferry (Tables 10 and 11, Figures 12 and 13), both in bias and rms for all coordinates. As for the baseline Digby–Ferry (Tables 10 and 11, Figures 14 and 15), NWM only marginally improves the statistics, with a worsening in height compared to UNB3m. Again, the observation residuals surprisingly show no significant change, even when we use no tropospheric model.

Table 10: Rms of observation residuals (in m); moving rover scenario.

		C/A Code	L1 Phase
St. John	no model	1.23	0.026
	Saastamoinen	1.22	0.020
	UNB3m	1.22	0.022
	NWM	1.23	0.021
Digby	no model	1.07	0.031
	Saastamoinen	1.05	0.016
	UNB3m	1.05	0.018
	NWM	1.05	0.018

Table 11: Statistics (in cm) for discrepancy between test and reference solutions, moving rover scenario.

		Height			Latitude			Longitude		
		mean	rms	std	mean	rms	std	mean	rms	std
St. John	no model	10.2	16.1	12.5	-8.1	10.2	6.2	-0.8	6.4	6.3
	Saastamoinen	2.4	10.5	10.2	-1.6	5.2	4.9	-2.8	5.1	4.3
	UNB3m	4.3	8.0	6.8	-1.9	4.8	4.4	-1.3	3.1	2.8
	NWM	1.5	5.8	5.6	-0.9	3.3	3.2	-0.8	2.8	2.6
Digby	no model	10.0	21.5	19.1	4.9	11.7	10.6	-5.6	11	9.4
	Saastamoinen	-1.9	5.9	5.5	0.3	4.1	4.1	1.0	2.3	2.0
	UNB3m	-0.5	8.4	8.4	-0.8	4.6	4.5	-1.5	4.0	3.7
	NWM	0.9	9.2	9.1	-0.6	4.3	4.2	-1.5	3.8	3.5

CONCLUSION

We have shown that NWM have only marginal improvement on a specific 70 km kinematic baseline over well-established tropospheric delay prediction models (Saastamoinen, UNB3m). As ray-tracing in NWM is far more complex and computationally more expensive than those simpler models, they should be preferred until one demonstrates that the impact of NWM tropospheric delay predictions is, indeed, far superior.

ONGOING AND FUTURE WORK

To introduce the predicted delays, currently we are (i) converting the receiver-specific observation files to RINEX and then (ii) subtracting the predicted delays from the raw observations, yielding corrected RINEX observation files. We are aware that this approach is not the best, in the sense that in (i) we may lose information about cycle slips already detected by the receiver itself, and in (ii) we may be introducing additional cycle slips. Therefore we are working to be able to introduce the predicted delays at the estimation level.

As future work, we plan to process a number of varying-length baselines (from, e.g., 50 up to 1,000 km). These will be stationary rovers processed in kinematic mode, so as to allow us to assess their accuracy by comparing the rover position solutions to their known static solutions.

Our aim is to determine the baseline length for which NWM tropospheric delay starts to be far superior to well-established, simpler tropospheric delay prediction models.

As a long-term goal, we would like to extend the analysis presented in this paper to yearlong sessions, so as to cover different seasons and anomalous atmospheric conditions.

ACKNOWLEDGMENTS

- Prof. Dr. Marcelo Santos, University of New Brunswick, for supervision;
- Mr. Rodrigo Leandro, University of New Brunswick, for fruitful discussions and also for providing the PPP solution and radiosonde ray-traces;
- NOAA for the radiosonde data;
- Canadian Meteorological Centre for the NWM;
- Geodetic Survey Division of NRCan for their PPP application;
- Canadian International Development Agency (CIDA) for funding;
- Office of Naval Research, through University of Southern Mississippi, and National Science and Engineering Research Council (NSERC), for financial support for the Princess of Acadia Project.

This research is inserted into GEOIDE Project “Next-Generation Algorithms for Next-generation algorithms for navigation, geodesy and earth sciences under modernized Global Navigation Satellite Systems.”

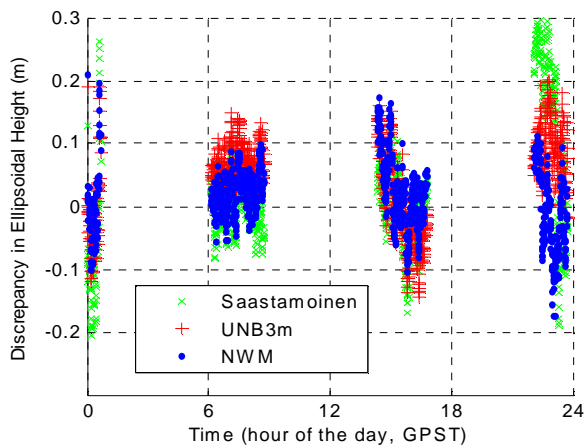


Figure 12: Time series of discrepancy in height; moving rover scenario, baseline St. John – Ferry.

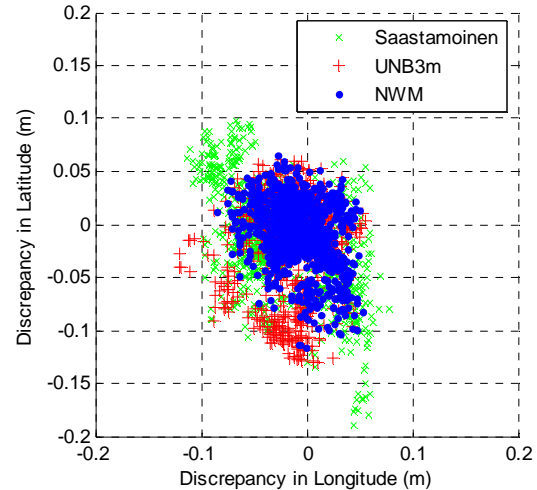


Figure 13: Horizontal discrepancy; moving rover scenario, baseline St. John – Ferry.

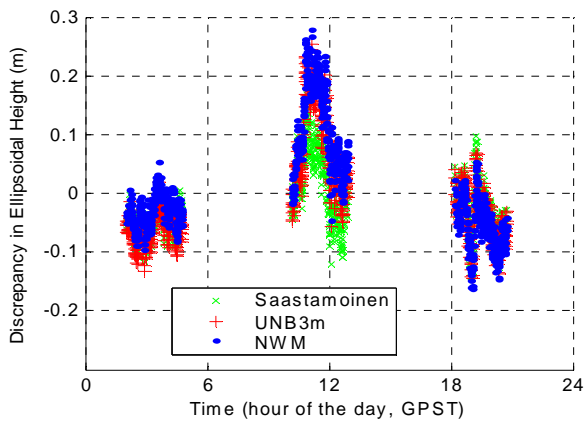


Figure 14: Time series of discrepancy in height; moving rover scenario, baseline Digby – Ferry.

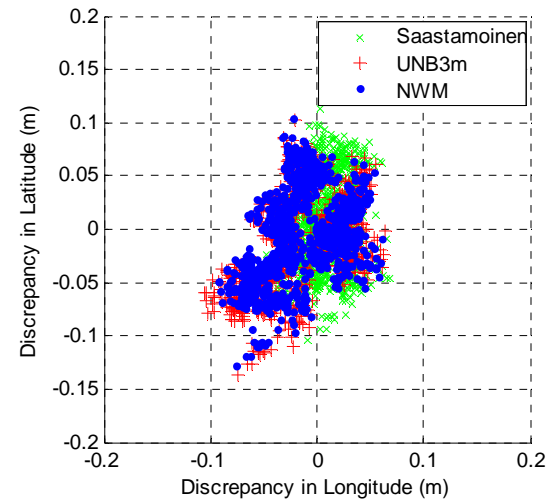


Figure 15: Horizontal discrepancy; moving rover scenario, baseline Digby – Ferry.

REFERENCES

Ahn, Y. W., G. Lachapelle, S. Skone, S. Gutman, and S. Sahn. Analysis of GPS RTK performance using external NOAA tropospheric corrections integrated with a multiple reference station approach. *GPS Solutions*, 10 (3): 171-186, July, 2006.

Böhm, J. and H. Schuh. Vienna Mapping Functions in VLBI analyses. *Geophys. Res. Lett.*, 31(L01603), 2004.

Cove, K., M. C. Santos, D. Wells and S. Bisnath (2004). Improved tropospheric delay estimation for long baseline, carrier phase differential GPS positioning in a coastal environment. *Proceedings of the Institute of Navigation*

GNSS-2004, 21-24 September, 2004, Long Beach, CA, USA, pp. 925-932.

Côté, J., S. Gravel, A. Méthot, A. Patoine, M. Roch, A. Staniforth (1998). The Operational CMC-MRB Global Environmental Multiscale (GEM) Model. Part I: Design Considerations and Formulation. *Monthly Weather Review*. Vol. 126, Issue: 6. pp. 1373-1395.

Cucurull, L., P. Sed, D. Behrend, E. Cardellach and A. Rius, Integrating NWP products into the analysis of GPS observables, *Physics and Chemistry of the Earth, Parts A/B/C*, Volume 27, Issues 4-5, 2002, pp. 377-383.

Dodson, A. H., W. Chen, N. T. Penna and H. C. Baker, GPS estimation of atmospheric water vapour from a moving platform, *Journal of Atmospheric and Solar-Terrestrial Physics*, Volume 63, Issue 12, August 2001, pp. 1331-1341.

Glickman, T.S. (ed.) *Glossary of meteorology*. 2nd ed. American Meteorological Society, Boston, 2000, 855 p.

Jensen, A.B.O. (2002) Investigations on the use of numerical weather predictions, ray tracing, and tropospheric mapping functions for network RTK. *Proceedings of the Institute of Navigation GPS-2002*, 24-27 September, 2002, Portland, OR, CA, USA, pp. 2324-2333.

Kouba, J. *A guide to using International GPS Service (IGS) products*. Publications of the IGS Central Bureau. February 2003.

Leandro, R., Santos, M., Langley, R. UNB Neutral Atmosphere Models: Development and Performance. *Proceedings of ION NTM 2006*, Monterey, CA, USA, Jan 18-20, 2006.

McCarthy, D.D. Petit, G. (2004) IERS Conventions (2003) (IERS Technical Note # 32). Frankfurt am Main: Verlag des Bundesamts für Kartographie und Geodäsie, 2004. 127 pp.

Mendes, V. B. (1999). *Modeling the Neutral-Atmosphere Propagation Delay in Radiometric Space Techniques*. Ph.D. dissertation, Department of Geodesy and Geomatics Engineering Technical Report No. 199, University of New Brunswick, Fredericton, New Brunswick, Canada, 353 pp.

Niell, A. E., 1996, "Global Mapping Functions for the Atmosphere Delay of Radio Wavelengths," *J. Geophys. Res.*, 101, pp. 3227-3246.

Nievinski, F., K. Cove, M. Santos, D. Wells, R. Kingdon. Range-Extended GPS Kinematic Positioning Using Numerical Weather Prediction Model, *Proceedings of ION AM 2005*, Cambridge, MA, USA, June 27-29, 2005.

Santos, M. C., D. Wells, K. Cove and S. Bisnath (2004). The Princess of Acadia GPS Project: Description and scientific challenges. *Proceedings of the Canadian Hydrographic Conference CHC2004*, 25-27 May, 2004, Ottawa.

Schüler, T. Impact of systematic errors on precise long-baseline kinematic GPS positioning, *GPS Solutions*, 10 (2): 108-125, Mar 2006.

Seeber, G. (2003) *Satellite geodesy: foundations, methods, and applications*. 2nd edition. Walter de Gruyter.